Accepted Manuscript

Synthesis and biological evaluation of quinazolin-4(3*H*)-one derivatives bearing dithiocarbamate side chain at C2-position as potential antitumor agents

Pan-Pan Ding, Man Gao, Bei-Bei Mao, Sheng-Li Cao, Cui-Huan Liu, Chao-Rui Yang, Zhong-Feng Li, Ji Liao, Hongchang Zhao, Zheng Li, Jing Li, Hailong Wang, Xingzhi Xu

PII: S0223-5234(15)30380-9

DOI: 10.1016/j.ejmech.2015.11.044

Reference: EJMECH 8234

To appear in: *European Journal of Medicinal Chemistry*

Received Date: 9 June 2015

Revised Date: 24 November 2015

Accepted Date: 25 November 2015

Please cite this article as: P.-P. Ding, M. Gao, B.-B. Mao, S.-L. Cao, C.-H. Liu, C.-R. Yang, Z.-F. Li, J. Liao, H. Zhao, Z. Li, J. Li, H. Wang, X. Xu, Synthesis and biological evaluation of quinazolin-4(3*H*)-one derivatives bearing dithiocarbamate side chain at C2-position as potential antitumor agents, *European Journal of Medicinal Chemistry* (2015), doi: 10.1016/j.ejmech.2015.11.044.

Synthesis and biological evaluation of quinazolin-4(3*H*)-one derivatives bearing dithiocarbamate side chain at C2-position as potential antitumor agents

Pan-Pan Ding[a], Man Gao[a], Bei-Bei Mao[a], Sheng-Li Cao[a*], Cui-Huan Liu[a], Chao-Rui Yang[a], Zhong-Feng Li[a], Ji Liao[b], Hongchang Zhao[b], Zheng Li[b], Jing Li[b], Hailong Wang[b], and Xingzhi Xu[b*]

[a] *Department of Chemistry, Capital Normal University, Beijing 100048, PR China*

[b] *Beijing Key Laboratory of DNA Damage Response, College of Life Science, Capital Normal University, Beijing 100048, PR China*

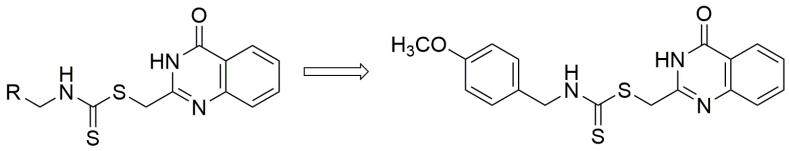

Compounds **5a**–**t** were synthesized and evaluated as antitumor agents. Among them, **5c** inhibited the proliferation of HT29 cells by interfering with tubulin, leading to a cell cycle arrest at G2/M phase.

Synthesis and biological evaluation of quinazolin-4(3*H*)-one derivatives bearing dithiocarbamate side chain at C2-position as potential antitumor agents

Pan-Pan Ding[a], Man Gao[a], Bei-Bei Mao[a], Sheng-Li Cao[a*], Cui-Huan Liu[a], Chao-Rui Yang[a], Zhong-Feng Li[a], Ji Liao[b], Hongchang Zhao[b], Zheng Li[b], Jing Li[b], Hailong Wang[b], Xingzhi Xu[b*]

[a] *Department of Chemistry, Capital Normal University, Beijing 100048, PR China*

[b] *Beijing Key Laboratory of DNA Damage Response, College of Life Science, Capital Normal University, Beijing 100048, PR China*

Abbreviations: 5-FU, 5-Fluorouracil; ATR, attenuated total reflection; BubR1, Bub1-related protein kinase; CPT, Camptothecin; 7,8-DHF, 7,8-dihydrofolate; DHFR, dihydrofolate reductase; DSB, DNA double-strand break; γ-H2AX, histone H2AX phosphorylated on serine 139; MTS, 3-(4,5-dimethylthiazol-2-yl)-5-(3-carboxymethoxyphenyl)-2-(4-sulfophenyl)-2*H*-tetrazolium, inner salt; NADPH, nicotinamide adenine dinucleotide phosphate; Noc, Nocodazole; TS, thymidylate synthase.

* Corresponding authors. Tel/fax: +86 10 68902974 (S. L. Cao), +86 10 68902240 (X. Xu).
E-mail address: slcao@cnu.edu.cn (S. L. Cao), xingzhi_xu@mail.cnu.edu.cn (X. Xu).

ABSTRACT: A series of quinazolin-4(3*H*)-one derivatives bearing dithiocarbamate side chain at the C2-position were synthesized and evaluated for their antiproliferative activities against A549, MCF-7, HeLa, HT29 and HCT-116 cell lines. Most of the synthesized compounds exhibited broad spectrum antitproliferative activity against five cell lines, of which **5c** was the most potent against HT29 cell line with an IC_{50} value of 5.53 μM, inducing a G2/M phase arrest in HT29 cells. Treatment of HT29 cells with **5c** resulted in BubR1 phosphorylation and an increase of mitotic index in a time-dependent manner. Furthermore, **5c** promoted tubulin polymerization *in vitro*. These results demonstrate that quinazolin-4(3*H*)-one derivatives bearing dithiocarbamate side chain at C2-position may be potentially novel antitumor agents targeting tubulin to activate the spindle assembly checkpoint.

Keywords: Quinazolin-4(3*H*)-one; dithiocarbamate; synthesis; antiproliferative activity; G2/M arrest; spindle assembly checkpoint.

1. Introduction

Quinazoline derivatives bearing side chains at the C5 or C6-position of the core structure possess promising antitumor property by targeting folate dependent enzymes including thymidylate synthase (TS) and dihydrofolate reductase (DHFR). TS catalyzes the reductive methylation of 2′-deoxyuridine-5′-monophosphate (dUMP) to 2′-deoxythymidine-5′-monophosphate (dTMP). This reaction requires 5,10-methylenetetrahydrofolate (5,10-CH_2THF) as the donor of the methyl group, which is oxidized to 7,8-dihydrofolate (7,8-DHF). DHFR catalyzes the conversion of 7,8-DHF to 5,6,7,8-tetrahydrofolate (5,6,7,8-THF) using nicotinamide adenine dinucleotide phosphate (NADPH) as the reductant. Thus, TS and DHFR are crucial for the synthesis of dTMP in dividing cells, and TS and/or DHFR inhibitors have found clinical utility as antitumor agents [1,2]. The quinazoline skeleton is similar to the pteridine ring in folic acid molecule, and therefore its derivatives resembling the folic acid structure are of importance for the discovery of antitumor antifolates interfering with folate dependent enzymes.

The quinazoline derivatives containing L-glutamic acid moiety are generally referred to as classical antifolates such as ZD1694 [3] and CB3717 [4], while the derivatives containing lipophilic side chains are called non-classical antifolates such as AG337 [5] and Trimetrexate [6] (Fig. 1). Several classical or non-classical antifolates have been approved for clinical use or entered clinical trials [1,2]. In our attempts to explore quinazoline-based antitumor agents, the dithiocarbamate moiety that has been recognized as an efficient antitumor pharmacophore [7-9] was incorporated into the C6-position of 2-methylquinazlin-4(3*H*)-one as a lipophilic side chain. Among the synthesized compounds, **I** and **II** (Fig. 1) inhibited the proliferation of several human cancer cell lines with IC_{50} values at the level of micromolar concentrations [10-12].

Recently, increasing evidences indicate that quinazlin-4(3*H*)-one derivatives carrying various substituents at the C2-position can also exert inhibitory effects on tumor cells. Nevertheless, they may act through the mechanism of action different from that of quinazoline-based antifolates. For example, Ispinesib (Fig. 2), a kinesin spindle protein inhibitor, causes mitotic arrest and growth inhibition in several human tumor cell lines and is currently tested in multiple phase II clinical trials [13]. Compound **III** (Fig. 2) inhibits the growth of human MCF-7 breast carcinoma cells and Burkitt lymphoma CA46 cells with IC_{50} values of 0.34 and 1.0 μM, respectively. At 3.4 μM, it caused disruption of the cellular microtubule system of the MCF-7 cells, while at 10 μM it induced G2/M arrest in Burkitt cells. These cellular effects are consistent with its mechanism of action resulting from its inhibitory effect on tubulin assembly [14]. These facts and our previous work motivated us to synthesize a new series of compounds **5a**–**t** (Fig. 2) by incorporating the dithiocarbamate moiety into the C2-position of quinazlin-4(3*H*)-one. The target compounds would be evaluated for their antiproliferative activity against human cancer cell lines and investigated the possible mechanism of action.

2. Chemistry

As outlined in Scheme 1, heating 2-aminobenzoic acid (**1**) in acetic anhydride under reflux yielded 2-methyl-4*H*-benzo[*d*][1,3]oxazin-4-one (**2**), which was directly used in the next step without purification. Reaction of **2** with 25% aqueous ammonia in ethanol gave 2-methylquinazolin-4(3*H*)-one (**3**). According to the reported method [15], bromination of **3** with *N*-bromosuccinimide (NBS) generated 2-(bromomethyl)quinazolin-4(3*H*)-one (**4**), which reacted with carbon disulfide and various arylmethylamines or heterocyclylmethylamines in the presence of potassium phosphate [16,17] to

afford quinazolin-4(3*H*)-one derivatives bearing dithiocarbamate side chain at the C2-position *viz*., target compounds **5a**–**t**.

3. Biology

The MTS [3-(4,5-dimethylthiazol-2-yl)-5-(3-carboxymethoxyphenyl)-2-(4-sulfophenyl)-2*H*-tetrazolium, inner salt] cell proliferation assay was used to evaluate the antiproliferative activity of the synthesized compounds against five human cancer cell lines including A549 (lung cancer), MCF-7 (breast adenocarcinoma), HeLa (cervical carcinoma), HT29 and HCT-116 (colorectal cancer). The inhibition of cell proliferation was determined 72 h after cells were exposed to the tested compounds at a concentration of 50 μM. The compounds with 50% or more inhibition compared with vehicle-treated cells were considered active. Inhibition of cell proliferation by these active compounds at various concentrations were further measured, and their IC_{50} (the concentration that causes 50% of cell proliferation inhibition) values were determined and summarized in Table 1. 5-Fluorouracil (5-FU) was used as a positive control.

Among the tested compounds, **5c** exhibited significant antiproliferative activity against HT29 cells with an IC_{50} value of 5.53 μM. To gain further insight into the mechanisms of action of this new and active compound, we examined if treatment of HT29 cells with compound **5c** would lead to cell cycle arrest and DNA damage. HT29 cells were treated with compound **5c** or 5-FU at a concentration equivalent to its IC_{50} for 24 h. 5-FU is an inhibitor of TS, blocking DNA synthesis in a variety of cancer cells. Cells were harvested for cell cycle analysis by flow cytometry. Three independent experiments were performed, and the results were shown in Table 2. Meanwhile, indirect immunofluorescence assay and immuno-blotting analysis using antibody specific for the DNA double-strand break (DSB) marker γ-H2AX (histone H2AX phosphorylated on serine 139) were performed to examine whether these compounds would induce DSBs in cultured cancer cells. The results were demonstrated in Fig. 3. Mitotic index and BubR1 (Bub1-related protein kinase) phosphorylation levels were determined to assess the activation of the G2/M checkpoint or the spindle assembly checkpoint. The results were illustrated in Table 3 and Fig. 4. Furthermore, *in vitro* tubulin polymerization assays were conducted to evaluate if compound **5c** would interfere with tubulin polymerization *in vitro*, and the results were shown in Fig. 5.

4. Results and discussion

4.1. Antiproliferative activity

As shown in Scheme 1 and Table 1, we first synthesized compound **5a** (R = C_6H_5) to serve as a parent compound, which exhibited moderate antiproliferative activity against five cancer cell lines with IC_{50} values in the range of 10.70–31.33 μM. And then, compounds **5b**–**g** bearing electron-donating groups on the phenyl ring of the side chain were prepared and evaluated for their antiproliferative activity. Introduction of a methyl group into the 4-position of the phenyl ring (**5b**, R = 4-$CH_3C_6H_4$) led to a decrease in activity against four tumour cell lines. However, compound **5c** (R = 4-$CH_3OC_6H_4$) bearing a methoxyl group at the 4-position of the phenyl ring exhibited higher antiproliferative activity against A549 (7.27 versus 23.72 μM), MCF-7 (10.86 versus 31.33 μM) and HT29 (5.53 versus 14.45 μM) cell lines, and slightly weaker activity against HeLa and HCT-116 cell lines than the parent compound **5a**. In comparison with compound **5c**, **5d** (R = 2-$CH_3OC_6H_4$) was less active against each cell line, suggesting that a methoxyl group at the 4-position of the phenyl ring is favorable for the

antiproliferative activity. Compounds **5e** (R = 2,4-di$CH_3OC_6H_3$), **5f** (R = 3,4,5-tri$CH_3OC_6H_2$) and **5g** (R = 3,4-methylenedioxyC_6H_3) were in general less active than **5c**, indicating that one methoxyl group at the 4-position of the phenyl ring is adequate for generating the antiproliferative activity.

As for compounds bearing electron-withdrawing groups on the phenyl ring, compound **5h** (R = 4-BrC_6H_4) was less active than the parent compound **5a**, whereas **5i** (R = 4-ClC_6H_4) was inactive against five tumor cell lines. In contrast with **5e** versus **5c**, **5j** bearing two chlorine atoms at both the 2 and 4-position of the phenyl ring was more active against A549, HeLa, HT29 and HCT-116 cell lines than **5i** with one chlorine atom at the 4-position. Furthermore, compound **5k** (R = 4-FC_6H_4) bearing a fluorine atom at the 4-position of the phenyl ring was more potent than its 4-bromo or 4-chloro counterparts **5h** and **5i**. However, compounds **5l** (R = 2-FC_6H_4) and **5m** (R = 2,4-diFC_6H_3) exhibited lower or comparable activity to the 4-fluoro substituted compound **5k**, which IC_{50} was similar to compounds **5d**, **5e** and **5c**. In addition, compound **5n** bearing a stronger electron-withdrawing nitro group possessed comparable activity to **5k**, although both of them were less active than **5c** against four tumour cell lines. These results suggest that the electronic and steric characters of the substituent are not the critical determinant of activity.

Replacement of the phenyl group in the parent compound **5a** by thiophenyl, furanyl or pyridinyl group resulted in compounds **5o**–**t**. Compound **5o** (R = thiophen-2-yl) exhibited comparable activity against A549, HT29 and HCT-116 cell lines to compound **5a**, but higher activity against MCF-7 or lower activity against HeLa cell line than compound **5a**. Compound **5p** (R = furan-2-yl) was less active against each cell line than **5a**, while **5q** (R = pyridin-2-yl) was inactive at the concentration of 50 μM. Contrary to **5q**, compounds **5r** (R = pyridin-3-yl) and **5t** (R = pyridin-4-yl) exhibited higher activity against A549, MCF-7 and HCT-116 cell lines than **5a**, or comparable activity against HeLa, and HT29 cell lines to **5a**. In addition, the antiproliferative activity of **5s** bearing an electron-withdrawing group (trifluoromethyl) at the 6-position of the pyridine ring was close to its counterpart **5r**. These results indicate that the orientation of a heterocyclic substituent is crucial to the antiproliferative activity, while the density of electron cloud on the heterocycles exerts little effect on the activity.

Among the compounds synthesized, **5t** was the most active member with IC_{50} values of 6.13 and 16.67 μM against A549 and HCT-116 cell lines, respectively, whereas **5c** was the most potent one against HT29 cell line. Both compounds are worthy to be considered as leads for further studies. Since **5c** was more potent than the clinically used anticancer drug 5-FU against HT29 cells (5.53 versus 24.50 μM), it would be used for further investigation on the mechanism of action.

*4.2. Compound **5c** induced G2/M arrest in HT29 cells*

From the MTS assay results, we found that compound **5c** inhibited the proliferation of HT29 cells with an IC_{50} value of 5.53 μM. To reveal the molecular mechanism of **5c**-induced cytotoxicity, we determined the cell cycle profile of HT29 cells upon treatment with **5c**. HT29 cells were treated with compound **5c**, 5-FU at the concentrations equivalent to their IC_{50}, or Taxol (0.18 μM) for 24 h, and data were shown in Table 2. In agreement with previous reports, HT29 cells treated with 5-FU or Taxol for 24 h were arrested in S-phase or G2/M phase, respectively; while treatment with compound **5c** for 24 h only induced a G2/M arrest in HT29 cells without an obvious sub-G1 peak in the cell cycle profile.

*4.3. Compound **5c** did not induce DNA damage in HT29 cells*

Given that compound **5c** induces the G2/M arrest in HT29 cells, one of its potential mechanisms is that it induces DNA damage. To test this possibility, we treated HT29 cells with Camptothecin (CPT, 2

μM) or compound **5c** for 1 or 2 h. And then, indirect immunofluorescence assay and immuno-blotting analysis using antibody specific for the DSB marker γ-H2AX were performed to examine whether these compounds would induce DSBs in cultured cancer cells. The results were demonstrated in Fig. 3. CPT is an inhibitor of topoisomerase I, which induces replication-dependent DNA damage. We found that treatment with CPT, but not compound **5c**, resulted in distinct γ-H2AX focus formation by immunofluorescence staining analysis and an increase of γ-H2AX protein levels (Fig. 3). It has been well established that γ-H2AX is a marker for DSBs [18-20]. These results indicated that compound **5c** might not be able to induce DNA damage.

*4.4. Compound **5c** activated the spindle assembly checkpoint*

A G2/M arrest may result from DNA damage-induced G2/M checkpoint activation or tubulin poison-induced spindle assembly checkpoint activation. Given that compound **5c** failed to induce DNA damage, we sought to determine if compound **5c** would activate the spindle assembly checkpoint to elicit the G2/M arrest. To this end, we determined the mitotic indexes of HT29 cells treated with 5-FU, CPT, Noc or compound **5c** for different periods of time. The mitotic index was determined by the percentage of cells positive of immunostaining with the phospho-Histone H3 on serine 10 (H3S10) antibody. The H3S10 phosphorylation starts at prophase and quickly disappears when cells move from metaphase to anaphase. Both Noc and Taxol elicit their function in the spindle assembly checkpoint activation mainly through binding to tubulin and arresting cells at metaphase. The former leads to destabilization of tubulin polymerization, while Taxol treatment increases polymerization of tubulin units. As shown in Table 3, 5-FU treatment reduced the mitotic index because it arrested cells at the S phase, CPT treatment reduced the mitotic index as well since it activated the G2/M checkpoint to prevent the mitotic entry, while Noc treatment led to a continuing increase of mitotic index between the 2 hour time point and the 16 hour time point. Compound **5c** treatment resulted in a similar, but less extent, continuing increase of mitotic indexes (Table 3). As presented in Fig. 4, Taxol treatment increased phospho-BubR1 levels, while a less extent increase of BubR1 phosphorylation levels was seen when cells were treated with compound **5c** for the same period of time. BubR1 is a mitotic regulatory kinase that ensures accurate segregation of chromosomes through its role in the mitotic checkpoint and the establishment of proper microtubule-kinetochore attachments. BubR1 phosphorylation is an indicator of the spindle assembly checkpoint activation [21,22]. Taken together, these results demonstrated that compound **5c** activates the spindle assembly checkpoint.

*4.5. Compound **5c** promoted tubulin polymerization in vitro*

Finally, *in vitro* tubulin polymerization assays were conducted to evaluate if compound **5c** would interfere with tubulin polymerization *in vitro*, and the results were shown in Fig. 5. The *in vitro* tubulin polymerization assay confirmed that Taxol eliminated the nucleation phase and shortened the time for tubulin polymerization *in vitro* to reach the plateau (i.e., Vmax) in comparison to control. Compound **5c** reduced the nucleation phase in comparison to the control, while enhanced Vmax of the growth phase of tubulin polymerization *in vitro* in comparison to Taxol. These data indicate that compound **5c** may target tubulin and promote tubulin polymerization *in vitro*. Further investigation to uncover the biochemical and molecular mechnism how compund **5c** binds to tubulin and promotes its polymerization is warranted.

Introduction of new moieties into the C2-position of quinazoline has led to series of novel anticancer compounds. For examples, Ispinesib, a kinesin spindle protein inhibitor, is in phase II

clinical trials [13], while compound **III** exhibits its cytotoxic effect in cancer cells by inhibiting tubulin polymerization[14]. Our newly synthesized quinazolin-4(3*H*)-one derivatives bearing dithiocarbamate side chain at C2-position, compound **5c** in particular, elicit cytotoxic effects in different cancer cells by promoting tubulin polymerization and consequently activating the spindle assembly checkpoint. Therefore, exploration of C2-derivatives of quinazoline may yield promising anticancer compounds targeting G2/M phase of the cell cycle.

5. Conclusion

By transferring the dithiocarbamate side chain from the C6-position to the C2-position of quinazolin-4(3*H*)-one, a new series of compounds **5a–t** were designed and synthesized, and most of them exhibited antiproliferative activities against A549, MCF-7, HeLa, HT29 and HCT-116 cell lines. Among the active compounds, **5c** significantly inhibited the proliferation of HT29 cells with an IC_{50} value of 5.53 μM and induced a G2/M arrest by promoting tubulin polymerization *in vitro* and subsequently activating the spindle assembly checkpoint. These results have demonstrated that the potential target of compound **5c** is tubulin. How compound **5c** binds to tubulin and promotes its polymerization warrants further exploration.

6. Experimental

6.1. Chemistry

Melting points were determined on an XT5B microscopic melting point apparatus and are uncorrected. ^{1}H NMR spectra were recorded on a Varian VNMRS-600 spectrometer at 600 MHz using tetramethylsilane (TMS) as internal standard (Abbreviations: Ph = phenyl, Quin = quinazolin-4(3*H*)-one). ^{13}C NMR spectra were recorded on a Varian VNMRS-600 spectrometer at 150 MHz using tetramethylsilane (TMS) as internal standard. Infrared (IR) spectra were recorded on a Bruker Tensor 27 spectrometer with an ATR (attenuated total reflection) accessory. High-resolution electrospray ionization (HR-ESI) mass spectra were recorded on a Thermo Scientific LTQ Orbitrap Discovery (Bremen, Germany) mass spectrometer. Column chromatography was carried out on silica gel (200–300 mesh). High performance liquid chromatography (HPLC) analyses were performed on an Agilent 1200 Series HPLC instrument with a G1314B VWD (variable-wavelength detector) detector, and the results were presented in the Supplement materials. Arylmethylamines or heterocyclylmethylamines were obtained commercially and used without further purification.

*6.1.1. Preparation of 2-methylquinazolin-4(3H)-one (**3**)*

A mixture of 2-aminobenzoic acid (**1**) (1.37 g, 10 mmol) and acetic anhydride (10 mL) was stirred under reflux for 2 h. Most of excess acetic anhydride was removed by rotary evaporation and the residue was cooled to room temperature. The separated solid was filtered and dried to give 1.47 g of 2-methyl-4*H*-benzo[*d*][1,3]oxazin-4-one (**2**) as a yellow solid, which was used directly in the next step without purification.

A solution of **2** (1.47 g, 9.1 mmol) and 25% aqueous ammonia (37 mL) in ethanol (20 mL) was stirred at room temperature for 48 h. After removing most of the solvent and cooling, the precipitate was collected by filtration and dried in air, which was purified by recrystallization from ethanol to give 1.12 g (70%, overall yield of two steps) of **3** as a white solid, mp 233–236 °C (Lit. [23] mp 237–239 °C). ^{1}H NMR (600 MHz, DMSO-d_6) δ: 2.61 (s, 2H, CH_3), 7.65 (t, J = 7.8 Hz, 1H, Quin 6-H), 7.83 (d, J = 7.8 Hz, 1H, Quin 8-H), 7.96 (t, J = 7.8 Hz, 1H, Quin 7-H), 8.16 (d, J = 7.8 Hz, 1H, Quin

5-H). ^{13}C NMR (150MHz, DMSO-d_6) δ: 21.11, 49.02, 120.69, 125.20, 126.37, 126.91, 135.18, 156.22, 161.61. IR (ATR, cm^{-1}) ν: 3409, 3036, 2872, 2785, 1657, 1608, 1464, 1385, 1319, 1138, 942, 873, 771, 691. ESI-HRMS *m/z*: calcd for $C_9H_9N_2O$ ([M+H]$^+$): 161.0715; found: 161.0709.

*6.1.2. Preparation of 2-(bromomethyl)quinazolin-4(3H)-one (**4**)*

A stirred solution of 2-methylquinazolin-4(3*H*)-one (**3**) (6.40 g, 40 mmol), NBS (7.12 g, 40 mmol) in anhydrous DMF (35 mL) was heated at 40 °C for 24 h. The formed solid was collected by filtration and washed with ether and dry to give 7.37 g (77%) as a white solid, mp 227–230 °C. ^{1}H NMR (600 MHz, DMSO-d_6) δ: 4.41 (s, 2H, CH_2Br), 7.55 (t, *J* = 7.8 Hz, 1H, Quin 6-H), 7.67 (d, *J* = 7.8 Hz, 1H, Quin 8-H), 7.84 (t, *J* = 7.8 Hz, 1H, Quin 7-H), 8.12 (d, *J* = 7.8 Hz, 1H, Quin 5-H), 12.57 (br s, 1H, NH). ^{13}C NMR (150MHz, DMSO-d_6) δ: 30.18, 121.54, 126.28, 127.66 (2C), 135.06, 148.76, 153.27, 161.94. IR (ATR, cm^{-1}) ν: 3037, 2887, 2799, 1683, 1609, 1463, 1323, 1148, 897, 772, 674. ESI-HRMS *m/z*: calcd for $C_9H_8BrN_2O$ ([M+H]$^+$): 238.9820, 240.9800; found: 238.9813, 240.9790.

*6.1.3. General procedure for the preparation of compounds **5a–t***

A suspension of amine (1.5 mmol), carbon disulfide (0.6 mL, 10 mmol), and finely powdered potassium phosphate (0.40 g, 1.9 mmol) in DMF (20 mL) was stirred at room temperature for 0.5 h. After adding 2-(bromomethyl)quinazolin-4(3*H*)-one (**4**) (0.36 g, 1.5 mmol), stirring was continued for 1–3 h (for **5a-c**, **5h-n**, 1 h; for **5d-g**, 2 h; for **5o-t**, 3 h). The mixture was poured into water (150 mL) and the resulting precipitate was collected by filtration, dried in air. The crude product was purified by column chromatograph on silica gel using the solvent indicated below as eluent to give compounds **5a**–**t**.

*6.1.3.1. (4-Oxo-3,4-dihydroquinazolin-2-yl)methyl benzylcarbamodithioate (**5a**)*

Yield 63%, yellowish solid, mp 172–174 °C (eluent: CH_2Cl_2). ^{1}H NMR (600 MHz, DMSO-d_6) δ: 4.45 (s, 2H, SCH_2), 4.85 (d, *J* = 5.4 Hz, 2H, C*H*$_2$NH), 7.29 (m, 1H, Ph 4'-H), 7.33 (m, 4H, Ph 2'-H, 3'-H, 5'-H, 6'-H), 7.42 (d, *J* = 7.8 Hz, 1H, Quin 8-H), 7.49 (t, *J* = 7.8 Hz, 1H, Quin 6-H), 7.77 (t, *J* = 7.8 Hz, 1H, Quin 7-H), 8.09 (d, *J* = 7.8 Hz, 1H, Quin 5-H), 10.70 (t, *J* = 5.4 Hz, 1H, CH_2N*H*), 12.41 (s, 1H, NH). ^{13}C NMR (150MHz, DMSO-d_6) δ: 37.91, 50.28, 121.38, 126.26, 127.06, 127.19, 127.77, 128.23 (2C), 128.86 (2C), 134.91, 137.38, 148.62, 153.89, 161.82, 195.52. IR (ATR, cm^{-1}) ν: 3179, 2920, 2874, 1665, 1604, 1549, 1401, 1319, 926, 903, 765, 695. ESI-MS *m/z*: 342 [M+H]$^+$. ESI-HRMS *m/z*: calcd for $C_{17}H_{16}N_3OS_2$ ([M+H]$^+$): 342.0735; found: 342.0723.

*6.1.3.2. (4-Oxo-3,4-dihydroquinazolin-2-yl)methyl 4-methylbenzylcarbamodithioate (**5b**)*

Yield 51%, off-white solid, mp 186–187 °C (eluent: CH_2Cl_2/CH_3OH = 95:5). ^{1}H NMR (600 MHz, DMSO-d_6) δ: 2.29 (s, 3H, CH_3), 4.44 (s, 2H, SCH_2), 4.80 (d, *J* = 5.4 Hz, 2H, C*H*$_2$NH), 7.14 (d, *J* = 7.8 Hz, 2H, C_6H_4-H), 7.22 (d, *J* = 7.8 Hz, 2H, C_6H_4-H), 7.38 (d, *J* = 8.4 Hz, 1H, Quin 8-H), 7.49 (t, *J* = 7.8 Hz, 1H, Quin 6-H), 7.76 (t, *J* = 8.4 Hz, 1H, Quin 7-H), 8.09 (d, *J* = 7.8 Hz, 1H, Quin 5-H), 10.66 (t, *J* = 5.4 Hz, 1H, CH_2N*H*), 12.40 (s, 1H, NH). ^{13}C NMR (150MHz, DMSO-d_6) δ: 21.15, 37.90, 50.12, 121.37, 126.24, 127.06, 127.17, 128.30 (2C), 129.39 (2C), 134.29, 134.87, 136.98, 148.58, 153.94, 161.81, 195.23. IR (ATR, cm^{-1}) ν: 3139, 2919, 2811, 1673, 1610, 1524, 1468, 1401, 1316, 1075, 921, 807, 764, 683. ESI-HRMS *m/z*: calcd for $C_{18}H_{18}N_3OS_2$ ([M+H]$^+$): 356.0891; found: 356.0881.

*6.1.3.3. (4-Oxo-3,4-dihydroquinazolin-2-yl)methyl 4-methoxybenzylcarbamodithioate (**5c**)*

Yield 61%, yellowish solid, mp 178–179 °C (eluent: CH_2Cl_2/CH_3OH = 98:2). ^{1}H NMR (600 MHz, DMSO-d_6) δ: 3.74 (s, 3H, OCH_3), 4.43 (s, 2H, SCH_2), 4.77 (d, *J* = 5.4 Hz, 2H, C*H*$_2$NH), 6.89 (d, *J* = 8.4 Hz, 2H, C_6H_4 3'-H, 5'-H), 7.27 (d, *J* = 8.4 Hz, 2H, C_6H_4 2'-H, 6-H), 7.39 (d, *J* = 7.8 Hz, 1H, Quin

8-H), 7.49 (t, *J* = 7.8 Hz, 1H, Quin 6-H), 7.76 (t, *J* = 7.8 Hz, 1H, Quin 7-H), 8.08 (d, *J* = 7.8 Hz, 1H, Quin 5-H), 10.63 (t, *J* = 5.4 Hz, 1H, CH_2NH), 12.40 (s, 1H, NH). ^{13}C NMR (150MHz, DMSO-d_6) *δ:* 37.88, 49.89, 55.54, 114.22 (2C), 121.37, 126.25, 127.07, 127.18, 129.23, 129.79 (2C), 134.87, 148.58, 153.97, 159.09, 161.81, 194.99. IR (ATR, cm^{-1}) *ν*: 3137, 2896, 1672, 1616, 1511, 1404, 1304, 1247, 1073, 920, 848, 765. ESI-HRMS *m/z*: calcd for $C_{18}H_{18}N_3O_2S_2$ ([M+H]$^+$): 372.0840; found: 372.0831.

*6.1.3.4. (4-Oxo-3,4-dihydroquinazolin-2-yl)methyl 2-methoxybenzylcarbamodithioate (**5d**)*

Yield 49%, yellowish solid, mp 157–158 °C (eluent: CH_2Cl_2/CH_3OH = 98:2). ^{1}H NMR (600 MHz, DMSO-d_6) *δ*: 3.80 (s, 3H, OCH_3), 4.42 (s, 2H, SCH_2), 4.77 (d, *J* = 5.4 Hz, 2H, CH_2NH), 6.90 (t, *J* = 7.8 Hz, 1H, C_6H_4 5'-H), 7.03 (d, *J* = 7.8 Hz, 1H, C_6H_4 3'-H), 7.21 (d, *J* = 7.8 Hz, 1H, C_6H_4 6'-H), 7.30 (t, *J* = 7.8 Hz, 1H, C_6H_4 6'-H), 7.38 (d, *J* = 8.4 Hz, 1H, Quin 8-H), 7.50 (t, *J* = 8.4 Hz, 1H, Quin 6-H), 7.77 (t, *J* = 8.4 Hz, 1H, Quin 7-H), 8.09 (d, *J* = 8.4 Hz, 1H, Quin 5-H), 10.55 (t, *J* = 5.4 Hz, 1H, CH_2NH), 12.41 (s, 1H, NH). ^{13}C NMR (150MHz, DMSO-d_6) *δ:* 37.94, 46.04, 55.76, 111.23, 120.57, 121.35, 124.54, 126.26, 127.07, 127.13, 129.13, 129.28, 134.91, 148.56, 154.05, 157.41, 161.80, 195.16. IR (ATR, cm^{-1}) *ν*: 3173, 2922, 1672, 1610, 1462, 1321, 1243, 1079, 927, 749, 684. ESI-HRMS *m/z*: calcd for $C_{18}H_{18}N_3O_2S_2$ ([M+H]$^+$): 372.0840; found: 372.0833.

*6.1.3.5. (4-Oxo-3,4-dihydroquinazolin-2-yl)methyl 2,4-dimethoxybenzylcarbamodithioate (**5e**)*

Yield 51%, yellowish solid, mp 162–163 °C (eluent: CH_2Cl_2/CH_3OH = 98:2). ^{1}H NMR (600 MHz, DMSO-d_6) *δ*: 3.76 (s, 3H, OCH_3), 3.77 (s, 3H, OCH_3), 4.38 (s, 2H, SCH_2), 4.67 (d, *J* = 5.4 Hz, 2H, CH_2NH), 6.48 (dd, *J* = 8.4, 2.4 Hz, 1H, C_6H_3 5'-H), 6.59 (d, *J* = 2.4 Hz,1H, C_6H_3 3'-H), 7.15 (d, *J* = 8.4 Hz, 1H, C_6H_3 6'-H), 7.33 (d, *J* = 7.8 Hz, 1H, Quin 8-H), 7.50 (t, *J* = 7.8 Hz, 1H, Quin 6-H), 7.76 (t, *J* = 7.8 Hz, 1H, Quin 7-H), 8.09 (d,*J* = 7.8 Hz, 1H, Quin 5-H), 10.64 (t, *J* = 5.4 Hz,1H, CH_2NH), 12.40 (s, 1H, NH). ^{13}C NMR (150MHz, DMSO-d_6) *δ:* 37.94, 45.97, 55.70, 55.93, 98.86, 104.89, 116.65, 121.33, 126.25, 127.08, 127.10, 130.50, 134.87, 148.48, 154.18, 158.61, 160.81, 161.79, 194.56. IR (ATR, cm^{-1}) *ν*: 3162, 2923, 1671, 1625, 1536, 1508, 1465, 1417, 1317, 1208, 1156, 1127, 1070, 1038, 912, 773. ESI-HRMS *m/z*: calcd for $C_{19}H_{20}N_3O_3S_2$ ([M+H]$^+$): 402.0946; found: 402.0933.

*6.1.3.6. (4-Oxo-3,4-dihydroquinazolin-2-yl)methyl 3,4,5-trimethoxybenzylcarbamodithioate (**5f**)*

Yield 48%, yellowish solid, mp 168–170 °C (eluent: CH_2Cl_2/CH_3OH = 98:2). ^{1}H NMR (600 MHz, DMSO-d_6) *δ*: 3.64 (s, 3H, OCH_3), 3.70 (s, 6H, $2OCH_3$), 4.44(s, 2H, SCH_2), 4.76 (d, *J* = 4.8 Hz, 2H, CH_2NH), 6.68 (s, 2H, C_6H_2 2'-H, 6'-H), 7.34 (d, *J* = 7.8 Hz, 1H, Quin 8-H), 7.49 (t, *J* = 7.8 Hz, 1H, Quin 6-H), 7.74 (t, *J* = 7.8 Hz, 1H, Quin 7-H), 8.09 (d, *J* = 7.8 Hz, 1H, Quin 5-H), 10.64 (t, *J* = 4.8 Hz, 1H, CH_2NH), 12.42 (s, 1H, NH). ^{13}C NMR (150MHz, DMSO-d_6) *δ:* 37.93, 50.87, 56.26 (2C), 60.43, 105.99 (2C), 121.34, 126.26, 127.05, 127.09, 132.71, 134.85, 137.30, 148.53, 153.30 (2C), 154.10, 161.78, 195.25. IR (ATR, cm^{-1}) *ν*: 3250, 2980, 2920, 1690, 1609, 1464, 1340, 1314, 1250, 1119, 1004, 927, 764, 686. ESI-HRMS *m/z*: calcd for $C_{20}H_{22}N_3O_4S_2$ ([M+H]$^+$): 432.1052; found: 432.1038.

*6.1.3.7. (4-Oxo-3,4-dihydroquinazolin-2-yl)methyl 3,4-methylenedioxybenzylcarbamodithioate (**5g**)*

Yield 47%, yellowish solid, mp 176–177 °C (eluent: CH_2Cl_2/CH_3OH = 98:2). ^{1}H NMR (600 MHz, DMSO-d_6) *δ*: 4.43 (s, 2H, SCH_2), 4.74 (d, *J* = 4.8 Hz, 2H, CH_2NH), 6.0 (s, 2H, OCH_2O), 6.82 (d, *J* = 7.8 Hz, 1H, C_6H_3 6'-H), 6.86 (d, *J* = 7.8 Hz, 1H, C_6H_3 5'-H), 6.90 (s, 1H, C_6H_3 2'-H), 7.42 (d, *J* = 7.8 Hz, 1H, Quin 8-H), 7.49 (t, *J* = 7.8 Hz, 1H, Quin 6-H), 7.77 (t, *J* = 7.8 Hz, 1H, Quin 7-H), 8.08 (d, *J* = 7.8 Hz, 1H, Quin 5-H), 10.62 (t, *J* = 4.8 Hz, 1H, CH_2NH), 12.41 (s, 1H, NH). ^{13}C NMR (150MHz, DMSO-d_6) *δ:* 37.87, 50.13, 101.40, 108.55, 108.90, 121.36, 121.82, 126.24, 127.06, 127.15, 131.02, 134.88, 146.97, 147.71, 148.58, 153.92, 161.80, 195.18. IR (ATR, cm^{-1}) *ν*: 3132, 3037, 2905, 2812, 1674, 1619, 1529, 1498, 1401, 1318, 1251, 1075, 1004, 923, 864, 812, 763, 686. ESI-HRMS *m/z*: calcd for $C_{18}H_{16}N_3O_3S_2$ ([M+H]$^+$): 386.0633; found: 386.0622.

*6.1.3.8. (4-Oxo-3,4-dihydroquinazolin-2-yl)methyl 4-bromobenzylcarbamodithioate (**5h**)*

Yield 71%, yellowish solid, mp 192–193 °C (eluent: CH_2Cl_2/CH_3OH = 95:5). ^{1}H NMR (600 MHz, DMSO-d_6) δ: 4.43 (s, 2H, SCH_2), 4.80 (d, J = 5.4 Hz, 2H, CH_2NH), 7.26 (d, J = 8.4 Hz, 2H, C_6H_4 2'-H, 6'-H), 7.43 (d, J = 7.8 Hz, 1H, Quin 8-H), 7.47 (t, J = 7.8 Hz, Quin 6-H), 7.50 (d, J = 8.4 Hz, 2H, C_6H_4 3'-H, 5'-H), 7.76 (t, J = 7.8 Hz, 1H, Quin 7-H), 8.07 (d, J = 7.8 Hz, 1H, Quin 5-H), 10.67 (t, J = 5.4, 1H, CH_2N*H*), 12.40 (br s, 1H, NH). ^{13}C NMR (150MHz, DMSO-d_6) δ: 37.91, 49.46, 120.81, 121.38, 126.25, 127.06, 127.19, 130.37 (2C), 131.71 (2C), 134.88, 136.88, 148.62, 153.76, 161.80, 195.80. IR (ATR, cm^{-1}) ν: 3140, 2924, 1673, 1613, 1525, 1468, 1398, 1315, 1076, 1008, 923, 845, 803, 766, 681. ESI-HRMS *m/z*: calcd for $C_{17}H_{15}BrN_3OS_2$ ([M+H]$^+$): 419.9840, 421.9819; found: 419.9833, 421.9801.

*6.1.3.9. (4-Oxo-3,4-dihydroquinazolin-2-yl)methyl 4-chlorobenzylcarbamodithioate (**5i**)*

Yield 50%, pink solid, mp 188–190 °C (eluent: CH_2Cl_2/CH_3OH = 95:5). ^{1}H NMR (600 MHz, DMSO-d_6) δ: 4.45 (s, 2H, SCH_2), 4.84 (d, J = 5.4 Hz, 2H, CH_2NH), 7.33 (d, J = 8.4 Hz, 2H, C_6H_4 2'-H, 6'-H), 7.38 (d, J = 8.4 Hz, 2H, C_6H_4 3'-H, 5'-H), 7.45 (d, J = 7.8 Hz, 1H, Quin 8-H), 7.50 (t, J = 7.8 Hz, 1H, Quin 6-H), 7.78 (t, J = 7.8 Hz, 1H, Quin 7-H), 8.09 (d, J = 7.8 Hz, 1H, Quin 5-H), 10.69 (t, J = 5.4 Hz, 1H, CH_2N*H*), 12.41 (s, 1H, NH). ^{13}C NMR (150MHz, DMSO-d_6) δ: 37.93, 49.43, 121.39, 126.27, 127.07, 127.19, 128.80 (2C), 130.04 (2C), 132.34, 134.89, 136.46, 148.64, 153.78, 161.82, 195.81. IR (ATR, cm^{-1}) ν: 3141, 2922, 1675, 1616, 1524, 1399, 1314, 1079, 923, 846, 804, 764, 730, 682. ESI-HRMS *m/z*: calcd for $C_{17}H_{15}ClN_3OS_2$ ([M+H]$^+$): 376.0345, 378.0316; found: 376.0338, 378.0300.

*6.1.3.10. (4-Oxo-3,4-dihydroquinazolin-2-yl)methyl 2,4-dichlorobenzylcarbamodithioate (**5j**)*

Yield 57%, brown solid, mp 179–180 °C (eluent: CH_2Cl_2/CH_3OH = 98:2). ^{1}H NMR (600 MHz, DMSO-d_6) δ: 4.46 (s, 2H, SCH_2), 4.86 (d, J = 4.8 Hz, 2H, CH_2NH), 7.35 (d, J = 8.4 Hz, 1H, C_6H_3 6'-H), 7.39 (dd, J = 8.4, 1.8 Hz, 1H, C_6H_3 5'-H), 7.49 (d, J = 7.8 Hz, 1H, Quin 8-H), 7.51 (t, J = 7.8 Hz, 1H, Quin 6-H), 7.63 (d, J = 1.8 Hz, 1H, C_6H_3 3'-H), 7.79 (t, J = 7.8 Hz, 1H, Quin 7-H), 8.10 (d, J = 7.8 Hz, 1H, Quin 5-H), 10.66 (t, J = 4.8 Hz, 1H, CH_2N*H*), 12.43 (s, 1H, NH). ^{13}C NMR (150MHz, DMSO-d_6) δ: 37.99, 47.70, 121.39, 126.27, 127.07, 127.19, 127.74, 129.23, 131.16, 133.23, 133.67, 133.78, 134.90, 148.63, 153.69, 161.81, 196.32. IR (ATR, cm^{-1}) ν: 3151, 2924, 1676, 1617, 1535, 1466, 1404, 1318, 1079, 928, 812, 769, 684. ESI-HRMS *m/z*: calcd for $C_{17}H_{14}Cl_2N_3OS_2$ ([M+H]$^+$): 409.9955, 411.9926; found: 409.9944, 411.9911.

*6.1.3.11. (4-Oxo-3,4-dihydroquinazolin-2-yl)methyl 4-fluorobenzylcarbamodithioate (**5k**)*

Yield 64.9%, white solid, mp 167–169 °C (eluent: CH_2Cl_2/CH_3OH = 98:2). ^{1}H NMR (600 MHz, DMSO-d_6) δ: 4.45 (s, 2H, SCH_2), 4.83 (d, J = 5.4 Hz, 2H, CH_2NH), 7.16 (t, J = 8.4 Hz, 2H, C_6H_4 3'-H, 5'-H), 7.37 (dd, J = 8.4, 5.4 Hz, 2H, C_6H_4 2'-H, 6'-H), 7.45 (d, J = 7.8 Hz, 1H, Quin 8-H), 7.50 (t, J = 7.8 Hz, 1H, Quin 6-H), 7.78 (td, J = 7.8, 1.2 Hz, 1H, Quin 7-H), 8.09 (dd, J = 7.8, 1.2 Hz, 1H, Quin 5-H), 10.68 (t, J = 5.4 Hz, 1H, CH_2N*H*), 12.41 (s, 1H, NH). ^{13}C NMR (150MHz, DMSO-*d*6) δ: 37.92, 49.48, 115.61 (d, 2C, J = 21.0 Hz), 121.39, 126.27, 127.06, 127.18, 130.31 (d, 2C, J = 7.5 Hz), 133.60 (d, J = 3.0 Hz), 134.90, 148.63, 153.82, 161.82, 161.89 (d, J = 241.5 Hz), 195.60. IR (ATR, cm^{-1}) ν: 3144, 2920, 2870, 1671, 1608, 1507, 1400, 1318, 1222, 1077, 922, 854, 768, 661. ESI-HRMS *m/z*: calcd for $C_{17}H_{15}FN_3OS_2$ ([M+H]$^+$): 360.0641; found: 360.0631.

*6.1.3.12. (4-Oxo-3,4-dihydroquinazolin-2-yl)methyl 2-fluorobenzylcarbamodithioate (**5l**)*

Yield 69%, yellowish solid, mp 159–160 °C (eluent: CH_2Cl_2/CH_3OH = 98:2). ^{1}H NMR (600 MHz, DMSO-d_6) δ: 4.45 (s, 2H, SCH_2), 4.86 (d, J = 4.8 Hz, 2H, CH_2NH), 7.15 (t, J = 7.2 Hz, 1H, C_6H_4 3'-H), 7.21 (t, J = 9.0 Hz, 1H, C_6H_4 5'-H), 7.36 (m, 2H, C_6H_4 4'-H, 6'-H), 7.46 (d, J = 7.8 Hz, 1H, Quin 8-H), 7.50 (t, J = 7.8 Hz, 1H, Quin 6-H), 7.78 (td, J = 7.8, 1.2 Hz, 1H, Quin 7-H), 8.09 (dd, J = 7.8, 1.2 Hz, 1H, Quin 5-H), 10.66 (t, J = 4.8 Hz, 1H, CH_2N*H*), 12.41 (s, 1H, NH). ^{13}C NMR (150MHz, DMSO-d_6)

δ: 37.97, 44.33 (d, *J* = 4.1 Hz), 115.73 (d, *J* = 21.2 Hz), 121.39, 124.01 (d, *J* = 14.7 Hz), 124.80 (d, *J* = 3.3 Hz), 126.27, 127.06, 127.19, 130.01 (d, *J* = 8.0 Hz), 130.55 (d, *J* = 4.1 Hz), 134.92, 148.65, 153.82, 160.65 (d, *J* = 243.9 Hz), 161.82, 195.91. IR (ATR, cm^{-1}) *ν*: 3182, 2982, 1679, 1607, 1377, 1313, 1222, 1067, 923, 888, 758. ESI-HRMS *m/z*: calcd for $C_{17}H_{15}FN_3OS_2$ ($[M+H]^+$): 360.0641; found: 360.0630.

*6.1.3.13. (4-Oxo-3,4-dihydroquinazolin-2-yl)methyl 2,4-difluorobenzylcarbamodithioate (**5m**)*

Yield 78%, yellowish solid, mp 162–163 °C (eluent: CH_2Cl_2/CH_3OH = 95:5). ^{1}H NMR (600 MHz, DMSO-d_6) *δ*: 4.45 (s, 2H, SCH_2), 4.82 (d, *J* = 4.8 Hz, 2H, C*H*$_2$NH),7.05 (td, *J* = 8.4, 1.8 Hz, 1H, C_6H_3 3'-H), 7.25 (td, *J* = 9.9, 1.8 Hz, 1H, C_6H_3 5'-H), 7.43 (m, 1H, C_6H_3 6'-H), 7.50 (m, 2H, Quin 8-H, 6-H), 7.79 (t, *J* = 7.8 Hz, 1H, Quin 7-H), 8.09 (d, *J* = 7.8 Hz, 1H, Quin 5-H), 10.63 (t, *J* = 4.8 Hz, 1H, CH_2N*H*), 12.41 (s, 1H, NH). ^{13}C NMR (150MHz, DMSO-d_6) *δ:* 37.96, 43.88, 104.31 (t, *J* = 25.6 Hz), 111.81 (dd, *J* = 21.2, 3.6 Hz), 120.44 (dd, *J* = 15.0, 3.6 Hz), 121.38, 126.28, 127.07, 127.13, 131.87 (dd, *J* = 9.8, 5.7 Hz), 134.92, 148.60, 153.80, 160.72 (dd, *J* = 246.8, 12.6 Hz), 161.85, 162.20 (dd, *J* = 244.8, 12.0 Hz), 195.96. IR (ATR, cm^{-1}) *ν*: 3149, 2883, 2810, 1678, 1609, 1540, 1504, 1465, 1409, 1319, 1078, 922, 767, 686. ESI-HRMS *m/z*: calcd for $C_{17}H_{14}F_2N_3OS_2$ ($[M+H]^+$): 378.0546; found: 378.0539.

*6.1.3.14. (4-Oxo-3,4-dihydroquinazolin-2-yl)methyl 4-nitrobenzylcarbamodithioate (**5n**)*

Yield 41%, yellowish solid, mp 179–180 °C (eluent: CH_2Cl_2/CH_3OH = 98:2). ^{1}H NMR (600 MHz, DMSO-d_6) *δ*: 4.48 (s, 2H, SCH_2), 4.99 (d, *J* = 5.4 Hz, 2H, C*H*$_2$NH), 7.49 (m, 2H, Quin 8-H, 6-H), 7.52 (d, *J* = 8.4 Hz, 2H, C_6H_4 3'-H, 5'-H), 7.78 (t, *J* = 7.8 Hz, 1H, Quin 7-H), 8.09 (d, *J* = 7.8 Hz, 1H, Quin 5-H), 8.18 (d, *J* = 8.4 Hz, 2H, C_6H_4 2'-H, 6'-H), 10.79 (t, *J* = 5.4 Hz, 1H, CH_2N*H*), 12.43 (s, 1H, NH). ^{13}C NMR (150MHz, DMSO-d_6) *δ:* 37.98, 49.35, 121.40, 123.96 (2C), 126.27, 127.06, 127.23, 128.95 (2C), 134.88, 145.48, 147.06, 148.67, 153.60, 161.82, 196.55. IR (ATR, cm^{-1}) *ν*: 3168, 2927, 2852, 1666, 1612, 1515, 1337, 1316, 1080, 925, 852, 762, 680. ESI-HRMS *m/z*: calcd for $C_{17}H_{15}N_4O_3S_2$ ($[M+H]^+$): 387.0586; found: 387.0576.

*6.1.3.15. (4-Oxo-3,4-dihydroquinazolin-2-yl)methyl thiophen-2-ylmethylcarbamodithioate (**5o**)*

Yield 46%, yellowish solid, mp 176–178 °C (eluent: CH_2Cl_2/CH_3OH = 98:2). ^{1}H NMR (600 MHz, DMSO-d_6)*δ*: 4.44 (s, 2H, SCH_2), 5.02 (d, *J* = 3.0 Hz, 2H, C*H*$_2$NH), 6.99 (t, *J* = 4.2 Hz, 1H, thiophen-2-yl 4'-H), 7.10 (d, *J* = 2.4 Hz, 1H, thiophen-2-yl 3'-H), 7.44 (d, *J* = 4.8 Hz, 1H, thiophen-2-yl 5'-H), 7.48 (d, *J* = 7.8 Hz, 1H, Quin 8-H), 7.49 (t, *J* = 7.8 Hz, 1H, Quin 6-H), 7.77 (t, *J* = 7.8 Hz, 1H, Quin 7-H), 8.09 (d, *J* = 7.8 Hz, 1H, Quin 5-H), 10.75 (br s, 1H, CH_2N*H*), 12.41 (s, 1H, NH). ^{13}C NMR (150MHz, DMSO-d_6) *δ:* 37.94, 45.01, 121.38, 126.25, 126.38, 127.06 (2C), 127.24, 127.57, 134.92, 139.44, 148.64, 153.79, 161.81, 195.39. IR (ATR, cm^{-1}) *ν*: 3164, 2976, 2928, 2896, 1678, 1609, 1467, 1382, 1318, 1256, 1076, 1062, 1003, 925, 889, 855, 770, 705, 684. ESI-HRMS *m/z*: calcd for $C_{15}H_{14}N_3OS_3$ ($[M+H]^+$): 348.0299; found: 348.0293.

*6.1.3.16. (4-Oxo-3,4-dihydroquinazolin-2-yl)methyl (furan-2-yl)methylcarbamodithioate (**5p**)*

Yield 48%, yellowish solid, mp 166–168 °C (eluent: CH_2Cl_2/CH_3OH = 98:2). ^{1}H NMR (600 MHz, DMSO-d_6) *δ*: 4.40 (s, 2H, SCH_2), 4.80 (d, *J* = 5.4 Hz, 2H, NHC*H*$_2$), 6.36 (d, *J* = 3.0 Hz, 1H, furan-2-yl 3'-H), 6.40 (m, 1H, furan-2-yl 4'-H), 7.47 (m, 2H, Quin 6-H, 8-H), 7.60 (m, 1H, furan-2-yl 5'-H), 7.76 (td, *J* = 7.8, 1.8 Hz, 1H, Quin 7-H), 8.06 (dd, *J* = 7.8, 1.8 Hz, 1H, Quin 5-H), 10.64 (t, *J* = 5.4 Hz, 1H, CH_2N*H*), 12.38 (s, 1H, NH). ^{13}C NMR (150MHz, DMSO-d_6) *δ:* 37.94, 43.53, 109.21, 111.03, 121.36, 126.25, 127.06, 127.23, 134.93, 143.18, 148.60, 150.05, 153.90, 161.79, 195.63. IR (ATR, cm^{-1}) *ν*: 3182, 2987, 1681, 1609, 1468, 1377, 1328, 1185, 1086, 1008, 935, 890, 769, 750, 686. ESI-HRMS *m/z*: calcd for $C_{15}H_{14}N_3O_2S_2$ ($[M+H]^+$): 332.0527; found: 332.0519 .

*6.1.3.17. (4-Oxo-3,4-dihydroquinazolin-2-yl)methyl pyridin-2-ylmethylcarbamodithioate (**5q**)*

Yield 48%, yellowish solid, mp 147–149 °C (eluent: CH_2Cl_2/CH_3OH = 98:2). ^{1}H NMR (600 MHz,

DMSO-d_6)δ: 4.46 (s, 2H, SCH_2), 4.93 (d, J = 3.0 Hz, 2H, CH_2NH), 7.30 (m, 2H, pyridin-2-yl 3'-H, 5'-H),7.49 (d, J = 7.8 Hz, 1H, Quin 8-H), 7.53 (t, J = 7.8 Hz, 1H, Quin 6-H), 7.74 (d, J = 7.8 Hz, 1H, pyridin-2-yl 4'-H), 7.79 (t, J = 7.8 Hz, 1H, Quin 7-H), 8.09 (d, J = 7.8 Hz, 1H, Quin 5-H), 8.52 (d, J = 4.2 Hz, 1H, pyridin-2-yl 6'-H), 10.80 (br s, 1H, CH_2N*H*), 12.42 (s, 1H, NH). ^{13}C NMR (150MHz, DMSO-d_6) δ: 37.99, 51.92, 121.37, 122.09, 122.93, 126.26, 127.05, 127.23, 134.82, 134.92, 137.20, 149.53, 153.82, 156.63, 161.83, 196.11. IR (ATR, cm^{-1}) ν: 3178, 2895, 1680, 1609, 1467, 1376, 1329, 1246, 1101, 936, 889, 770, 687. ESI-HRMS *m/z*: calcd for $C_{16}H_{15}N_4OS_2$ ([M+H]$^+$): 343.0687; found: 343.0681.

*6.1.3.18. (4-Oxo-3,4-dihydroquinazolin-2-yl)methyl pyridin-3-ylmethylcarbamodithioate (**5r**)*

Yield 52%, yellowish solid, mp 180–182 °C (eluent: CH_2Cl_2/CH_3OH = 98:2).^{1}H NMR (600 MHz, DMSO-d_6) δ: 4.46 (s, 2H, SCH_2), 4.87 (d, J = 5.4 Hz, 2H, CH_2NH), 7.35 (m, 1H, pyridin-3-yl 5'-H), 7.48 (d, J = 7.8 Hz, 1H, Quin 8-H), 7.50 (t, J = 7.8 Hz, 1H, Quin 6-H), 7.72 (d, J = 7.8 Hz, 1H, pyridin-3-yl 4'-H), 7.78 (t, J = 7.8 Hz, 1H, Quin 7-H), 8.09 (d, J = 7.8 Hz, 1H, Quin 5-H), 8.49 (d, J = 7.8 Hz, 1H, pyridin-3-yl 6'-H), 8.56 (s, 1H, pyridin-3-yl 2'-H), 10.71 (t, J = 5.4 Hz, 1H, CH_2N*H*), 12.42 (s, 1H, NH). ^{13}C NMR (150MHz, DMSO-d_6) δ: 37.93, 47.82, 121.39, 123.96, 126.27, 127.06, 127.20, 133.08, 134.93, 136.00, 148.66, 148.95, 149.57, 153.73, 161.82, 195.99. IR (ATR, cm^{-1}) ν: 3150, 2966, 2930, 1704, 1609, 1541, 1468, 1406, 1321, 1082, 924, 770, 715, 687. ESI-HRMS *m/z*: calcd for $C_{16}H_{15}N_4OS_2$ ([M+H]$^+$): 343.0687; found: 343.0682.

*6.1.3.19. (4-Oxo-3,4-dihydroquinazolin-2-yl)methyl (6-(trifluoromethyl)pyridin-3-yl)methylcarbamodithioate (**5s**)*

Yield 50%, yellowish solid, mp 164–166 °C (eluent: CH_2Cl_2/CH_3OH = 98:2). ^{1}H NMR (600 MHz, DMSO-d_6) δ: 4.48 (s, 2H, SCH_2), 4.97 (s, 2H, CH_2NH), 7.50 (m, 2H, Quin 8-H, 6-H), 7.77 (t, J = 7.8 Hz, 1H, Quin 7-H), 7.87 (d, J = 7.8 Hz, 1H, pyridin-3-yl 5'-H), 7.97 (d, J = 7.8 Hz, 1H, pyridin-3-yl 4'-H), 8.09 (d, J = 7.8 Hz, 1H, Quin 5-H), 8.73 (s, 1H, pyridin-3-yl 2'-H), 10.79 (s, 1H, CH_2N*H*), 12.42 (s, 1H, NH). ^{13}C NMR (150MHz, DMSO-d_6) δ: 37.97, 47.32, 120.95 (q, J = 2.5 Hz), 121.41, 122.1 (q, J = 271.5 Hz), 126.27, 127.06, 127.21, 134.88, 137.26, 137.77, 145.74 (q, J = 33.5 Hz), 148.66, 150.01, 153.59, 161.82, 196.57. IR (ATR, cm^{-1}) ν: 3144, 2929, 2875, 1679, 1614, 1327, 1176, 1134, 1085, 927, 855, 772. ESI-HRMS *m/z*: calcd for $C_{17}H_{14}F_3N_4OS_2$ ([M+H]$^+$): 411.0561; found: 411.0552.

*6.1.3.20. (4-Oxo-3,4-dihydroquinazolin-2-yl)methyl pyridin-4-ylmethylcarbamodithioate (**5t**)*

Yield 50%, yellowish solid, mp 148–150 °C (eluent: CH_2Cl_2/CH_3OH = 98:2). ^{1}H NMR (600 MHz, DMSO-d_6)δ: 4.48 (s, 2H, SCH_2), 4.88 (d, J = 4.8 Hz, 2H, CH_2NH), 7.27 (d, J = 4.8 Hz, 2H, pyridin-4-yl 3'-H, 5'-H), 7.52 (m, 2H, Quin 8-H, 6-H), 7.80 (t, J = 7.8 Hz, 1H, Quin 7-H), 8.10 (d, J = 7.8 Hz, 1H, Quin 5-H), 8.73 (d, J = 4.8 Hz, 2H, pyridin-4-yl 2'-H, 6'-H), 10.75 (s, 1H, CH_2N*H*), 12.43 (s, 1H, NH). ^{13}C NMR (150MHz, DMSO-d_6) δ: 37.96, 48.88, 121.40, 122.74 (2C), 126.29, 127.08, 127.23, 134.96, 146.48, 148.70, 150.01 (2C), 153.64, 161.84, 196.66. IR (ATR, cm^{-1}) ν: 3386, 2876, 2792, 1654, 1609, 1577, 1469, 1377, 1328, 1100, 933, 896, 773, 692, 634. ESI-HRMS *m/z*: calcd for $C_{16}H_{15}N_4OS_2$ ([M+H]$^+$): 343.0687; found: 343.0681.

6.2. Cell Proliferation Assay

Cell proliferation assay was performed as described [24]. Cell viability was tested with CellTiter 96® AQ_{ueous} One Solution Cell Proliferation Assay kit (Promega), based on the use of MTS. The data were obtained from triplicate wells in three independent experiments.

6.3. Distribution of HT29 cells in cell cycle and mitotic indexes evaluation

Cell cycle profiles were determined by propidium iodide staining and fluorescence-activated cell sorter analysis. Mitotic index was determined essentially as described previously [25] using phospho-Histone H3 (Ser-10) rabbit polyclonal antibodies (dilution 1:1000, Bethyl Laboratories, Inc).

6.4. Indirect immunofluorescence assay

Indirect immunofluorescence assay was performed as described before [26,27]. Mouse monoclonal antibody against γ-H2AX (clone JBW301) was purchased from Millipore and used in a dilution of 1:1500.

6.5. Immuno-blotting analysis

Immuno-blotting analysis was performed as described before [26,27]. Mouse monoclonal antibody against β-actin was from Sigma, and rabbit polyclonal antibodies against BubR1, γ-H2AX, Histone H3, and phospho-Histone H3 at Ser 10 (pH3S10) were purchased from Bethyl Laboratories, Inc and used at a dilution of 1:5000, 1:1000, 1:5000, 1:2000, and 1:1000, respectively.

6.6. Tubulin polymeration assay

In vitro tubulin polymerization assays were performed essentially as described by the manufacturer (Cytoskeleton, catalogue #BK006P). Polymerizations were monitored by an increase in absorbance at 340 nm over a 60 minute period at 37 °C. OD at 340 nm was determined using a SpectraMax M5 spectrometer (Molecular Devices).

Acknowledgements

This work was supported by the 973 project 2013CB911002, National Natural Science Foundation of China (Project No. 20972099, 31461143012 and 31130017), and Beijing Municipal Commission of Education (Project No. KZ201210028035).

References

[1] A. Gangjee, H.D. Jain, S. Kurup, Recent advances in classical and non-classical antifolates as antitumour and antiopportunistic infection agents: Part I, Anti-Cancer Agents Med. Chem. 7 (2007) 524–542.

[2] A. Gangjee, H.D. Jain, S. Kurup, Recent advances in classical and non-classical antifolates as antitumour and antiopportunistic infection agents: Part II, Anti-Cancer Agents Med. Chem. 8 (2008) 205–231.

[3] A.L. Jackman, F.T. Boyle, K.R. Harrap, Tomudex (ZD1694), from concept to care, a program in rational drug discovery, Invest. New Drugs 14 (1996) 305–316.

[4] T.R. Jones, A.H. Calvert, A.L. Jackman, S.T. Brown, M. Jones, K.R. Harrap, A potent antitumor quinazoline inhibitor of thymidylate synthase: synthesis, biological properties, and therapeutic results in mice, Eur. J. Cancer 17 (1981) 11–19.

[5] S. Webber, C.A. Bartlett, T.J. Boritzki, J.A. Hilliard, E.F. Howland, A.L. Johnston, M. Kosa, S.A. Margosiak, C.A. Morse, B.V. Shetty, AG337, a novel lipophilic thymidylate synthase inhibitor: *In vitro* and *in vivo* preclinical studies, Cancer Chemother. Pharmacol. 37 (1996) 509–517.

[6] A. Gangjee, W. Li, J. Yang, R.L. Kisliuk, Design, synthesis, and biological evaluation of classical and nonclassical 2-amino-4-oxo-5-substituted-6-methylpyrrolo[3,2-*d*]pyrimidines as dual thymidylate synthase and dihydrofolate reductase inhibitors, J. Med. Chem. 51 (2008) 68–76.

[7] P. Csomós, I. Zupkó, B. Réthy, L. Fodor, G. Falkay, G. Bernáth, Isobrassinin and its analogues: Novel types of antiproliferative agents, Bioorg. Med. Chem. Lett. 16 (2006) 6273–6276.

[8] X. Hou, Z. Ge, T. Wang, W. Guo, J. Cui, T. Cheng, C. Lai, R. Li, Dithiocarbamic acid esters as anticancer agent. Part 1: 4-Substituted-piperazine-1-carbodithioic acid 3-cyano-3,3-diphenyl-propyl esters, Bioorg. Med. Chem. Lett. 16 (2006) 4214–4219.

[9] M.A.-H. Zahran, T.A.-R.Salem, R.M. Samaka, H.S. Agwa, A.R. Awad, Design, synthesis and antitumour evaluation of novel thalidomide dithiocarbamate and dithioate analogs against Ehrlich ascites carcinoma-induced solid tumour in Swiss albino mice, Bioorg. Med. Chem. 16 (2008) 9708–9718.

[10] S.L. Cao, Y.P. Feng, Y.Y. Jiang, S.Y. Liu, G.Y. Ding, R.T. Li, Synthesis and *in vitro* antitumour activity of 4(3*H*)-quinazolinone derivatives with dithiocarbamate side chains, Bioorg. Med. Chem. Lett. 15 (2005) 1915–1917.

[11] S.L. Cao, Y.P. Feng, X.L. Zheng, Y.Y. Jiang, M. Zhang, Y. Wang, M. Xu, Synthesis of substituted-benzylamino- and heterocyclylmethylamino-carbodithioate derivatives of 4(3*H*)-quinazolinone and their cytotoxic activity, Arch. Pharm. 339 (2006) 250–254.

[12] S.L. Cao, Y. Wang, L. Zhu, J. Liao, Y.W. Guo, L.L. Chen, H.Q. Liu, X. Xu, Synthesis and cytotoxic activity of *N*-((2-methyl-4(3*H*)-quinazolinon-6-yl)methyl)dithiocarbamates, Eur. J. Med. Chem. 45 (2010) 3850–3857.

[13] L. Lad, L. Luo, J.D. Carson, K.W. Wood, J.J. Hartman, R.A. Copeland, R. Sakowicz, Mechanism of inhibition of human KSP by ispinesib, Biochemistry 47 (2008) 3576–3585.

[14] D. Raffa, M.C. Edler, G. Daidone, B. Maggio, M. Merickech, S. Plescia, D. Schillaci, R. Bai, E. Hamel, Synthesis, cytotoxicity, and inhibitory effects on tubulin polymerization of a new 3-heterocyclo substituted 2-styrylquinazolinones, Eur. J. Med. Chem. 39 (2004) 299–304.

[15] J. Bergman, A. Brynolf, Synthesis of chrysogine, a metabolite of penicillium chrysogenum and some related 2-substituted 4-(3*H*)-quinazolinones, Tetrahedron 46 (1990) 1295–1310.

[16] R.T. Li, P.Y. Ding, M. Han, M.S. Cai, A simple one-pot preparation of dithiocarbamates in the presence of anhydrous potassium phosphate, Synth. Commun. 28 (1998) 295–300.

[17] R.T. Li, Z.M. Ge, T.M. Cheng, M.S. Cai, New synthetic method for dithiocarbamates, Chem. J. Chin. Univ. 20 (1999) 1897–1902.

[18] E.P. Rogakou, D.R. Pilch, A.H. Orr, V.S. Ivanova, W.M. Bonner, DNA double-stranded breaks induce histone H2AX phosphorylation on serine 139, J. Biol. Chem. 273 (1998), 5858–5868.

[19] E.P. Rogakou, C. Boon, C. Redon, W.M. Bonner, Megabase chromatin domains involved in DNA double-strand breaks in vivo, J. Cell. Biol. 146 (1999), 905–915.

[20] T.T. Paull, E.P. Rogakou, V. Yamazaki, C.U. Kirchgessner, M. Gellert, W.M. Bonner, A critical role for histone H2AX in recruitment of repair factors to nuclear foci after DNA damage, Curr. Biol. 10 (2000), 886–895.

[21] W.Q. Li, Z.D. Lan, H.Y. Wu, S.C. Wu, J. Meadows, J. Chen, V. Zhu, W. Dai, BUBR1 phosphorylation is regulated during mitotic checkpoint activation, Cell Growth Differ. 10 (1999), 769–775.

[22] G.K.T. Chan, S.A. Jablonski, V. Sudakin, J.C. Hittle, T.J. Yen, Human BUBR1 is a mitotic checkpoint kinase that monitors CENP-E functions at kinetochores and binds the cyclosome/APC, J. Cell. Biol. 146 (1999), 941–954.

[23] S.A. Rocco, J.E. Barbarini, R. Rittner, Synthese of some 4-anilinoquinazoline derivatives, *Synthesis* (2004) 429–435.

[24] S. L. Cao, Y. Han, C. Z. Yuan, Y. Wang, Z. K. Xiahou, J. Liao, R. T. Gao, B. B. Mao, B. L. Zhao, Z. F. Li, X. Xu, Synthesis and antiproliferative activity of 4-substituted-piperazine-1-carbodithioate derivatives of 2,4-diaminoquinazoline, Eur. J. Med. Chem. 64 (2013) 401–409.

[25] X. Xu, J.H. Lee, D.F. Stern, Microcephalin is a DNA damage response protein involved in regulation of CHK1 and BRCA1, J. Biol. Chem. 279 (2004) 34091–34094.

[26] X. Xu, D.F. Stern, NFBD1/MDC1 regulates ionizing radiation-induced focus formation of DNA checkpoint signaling and repair factors, FASEB J. 17 (2003) 1842–1848.

[27] X. Xu, D.F. Stern, NFBD1/KIAA0170 is a chromatin-associated protein involved in DNA damage signaling pathways, J. Biol. Chem. 278 (2003) 8795–8803.

Figure captions

Fig. 1. Structures of ZD1694, CB3717, AG337, Trimetrexate and compounds **I**, **II**.

Fig. 2. Structures of Ispinesib, compound **III** and target compounds **5a**–**t**.

Fig. **3**. Compound **5c** does not induce DNA damage. (A) Compound **5c** failed to induce γ-H2AX foci formation. HT29 cell were treated with Camptothecin (CPT), compound **5c** or DMSO (dilutent for CPT and **5c**) for 1 or 2 h. Cells were fixed and immuno-stained with a mouse monoclonal antibody against γ-H2AX, and DNA was stained with 4',6-diamidino-2-phenylindole (DAPI). Scale bar: 20 μM. (B) Compound **5c** failed to increase γ-H2AX protein levels. HT29 cells were treated as described in (A), total lysates were harvested and immunoblotted with antibodies as indicated. Different sections from the same membrane were blotted with different antibodies according to the molecular weight of targeting antigens. The molecular weight of γ-H2AX and β-actin is 15 kDa and 42 kDa, respectively.

Fig. **4**. Compound **5c** induced BubR1 phosphorylation. After HT29 cells were treated with Taxol for 16 h or compound **5c** for 2, 4, 8, and 16 h, total lysates were harvested for immuno-blotting with antobsodies as indicated. Different sections from the same membrane were blotted with pH3S10, BubR1, and β-actin antibodies according to the molecular weight of targeting antigens, while the pH3S10 blot was striped and re-probed with an anti-Histone H3 antibody.

Fig. **5**. Compound **5c** promotes tubulin polymerization *in vitro*. *In vitro* tubulin polymerization assays were performed using purified porcine neuronal tubulin according to the manufacturer's instructions. I, II, and III denote the nucleation phase, the growth phase, and the steady state equilibrium phase of tubulin polymerization *in vitro*, respectively.

Scheme 1. Synthetic route to compounds **5a**–**t**. Reagents and conditions: (a) Ac_2O, reflux, 2 h. (b) 25% $NH_3 \cdot H_2O$, EtOH, rt, 48 h. (c) NBS, DMF, 40 °C, 24 h. (d) RCH_2NH_2, CS_2, K_3PO_4, DMF, rt, 1–3 h.

Table 1. Antiproliferative activity of compounds **5a–t** against five human cancer cell lines.

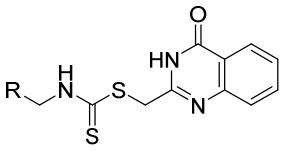

5a–t

Compound	R	IC_{50}[a], μM				
		A549	MCF-7	HeLa	HT29	HCT-116
5a	C_6H_5	23.72 ± 0.77	31.33 ± 1.27	10.70 ± 0.35	14.45 ± 1.28	18.12 ± 1.05
5b	4-$CH_3C_6H_4$	32.58 ± 0.75	21.36 ± 1.48	20.70 ± 0.89	16.34 ± 0.45	23.17 ± 1.46
5c	4-$CH_3OC_6H_4$	7.27 ± 0.75	10.86 ± 1.22	12.19 ± 0.60	5.53 ± 0.41	22.72 ± 3.20
5d	2-$CH_3OC_6H_4$	11.97 ± 1.40	14.84 ± 0.83	16.49 ± 0.56	12.28 ± 3.06	30.60 ± 1.80
5e	2,4-di$CH_3OC_6H_3$	10.47 ± 0.51	13.48 ± 0.64	15.99 ± 1.03	10.08 ± 0.54	25.47 ± 0.46
5f	3,4,5-tri$CH_3OC_6H_2$	10.42 ± 1.50	8.97 ± 0.57	22.95 ± 0.79	7.16 ± 0.96	17.31 ± 0.98
5g	3,4-MethylenedioxyC_6H_3	44.58 ± 2.86	21.66 ± 0.41	20.28 ± 0.21	19.27 ± 1.38	34.25 ± 1.47
h	4-BrC_6H_4	18.19 ± 1.68	39.17 ± 0.79	22.89 ± 0.50	32.27 ± 2.49	45.28 ± 4.82
5i	4-ClC_6H_4	> 50	> 50	> 50	> 50	> 50
5j	2,4-diClC_6H_3	12.83 ± 0.38	> 50	28.97 ± 2.12	11.37 ± 0.75	29.73 ± 3.12
5k	4-FC_6H_4	10.71 ± 0.31	17.36 ± 0.33	21.17 ± 0.76	18.57 ± 0.92	20.13 ± 0.13
5l	2-FC_6H_4	21.21 ± 1.57	20.49 ± 3.55	13.15 ± 0.59	16.42 ± 0.60	20.3 ± 1.90
5m	2,4-diFC_6H_3	30.58 ± 0.1	20.45 ± 1.30	20.05 ± 0.58	15.65 ± 1.38	22.31 ± 0.79
5n	4-$NO_2C_6H_4$	11.44 ± 1.50	19.28 ± 1.05	28.39 ± 0.89	17.21 ± 2.37	16.38 ± 2.64
5o	Thiophen-2-yl	25.67 ± 1.73	23.93 ± 1.33	26.12 ± 0.70	16.05 ± 0.84	16.09 ± 2.20
5p	Furan-2-yl	42.56 ± 1.95	> 50	31.20 ± 3.44	33.71 ± 2.61	24.62 ± 4.98
5q	Pyridin-2-yl	> 50	> 50	> 50	> 50	> 50
5r	Pyridin-3-yl	14.77 ± 1.63	20.23 ± 0.64	11.01 ± 2.13	14.21 ± 1.40	11.18 ± 0.29
5s	6-CF_3-pyridin-3-yl	12.87 ± 0.41	19.25 ± 2.13	28.43 ± 0.60	16.48 ± 1.15	16.66 ± 0.49
5t	Pyridin-4-yl	6.13 ± 1.04	16.08 ± 0.96	12.52 ± 2.48	15.98 ± 1.47	6.67 ± 0.85
5-FU		3.52 ± 0.46	32.18 ± 1.13	43.71 ± 3.49	24.50 ± 2.62	5.53 ± 0.90

[a] IC_{50}: The concentration that causes 50% of cell proliferation inhibition. Data are expressed as mean ± SD from triplicate determination from three independent experiments.

Table 2. Effects of compound **5c** on HT29 cell distribution in cell cycle.

Compound	Cell cycle distribution (%)[a]		
	G0/G1	S	G2/M
DMSO	50.25 ± 1.19	33.05 ± 2.22	16.7 ± 1.55
5-FU	5.42 ± 1.07	91.11 ± 0.81	3.48 ± 0.25
Taxol	1.7 ± 0.55	17.6 ± 6.57	80.71 ± 6.94
5c	16.45 ± 2.15	28.25 ± 3.82	55.31 ± 2.96

[a] Data are expressed as mean ± SD from triplicate determination from three independent experiments.

Table 3. Mitotic indexes of HT29 cells treated with compound **5c**.

Compound	Mitotic index[a]			
	2 h	4 h	8 h	16 h
DMSO	2.47 ± 0.71	3.13 ± 1.01	2.81 ± 0.82	2.87 ± 0.82
5-FU	2.28 ± 0.97	2.09 ± 1.08	0.29 ± 0.10	0.23 ± 0.12
CPT	1.55 ± 0.78	1.11 ± 0.67	0.33 ± 0.05	
Noc	5.22 ± 1.66	11.4 ± 3.8	25.61 ± 3.67	64.81 ± 3.54
5c	4.66 ± 1.99	7.75 ± 4.86	10.15 ± 1.83	37.85 ± 3.77

[a] Data are expressed as mean ± SD from triplicate determination from three independent experiments. The mitotic index for untreated cells was 2.94 ± 0.59.

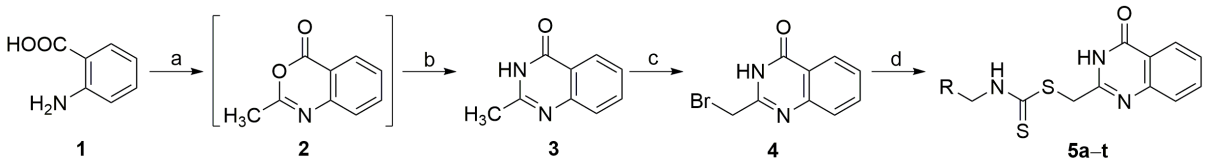

1 **2** **3** **4** **5a–t**

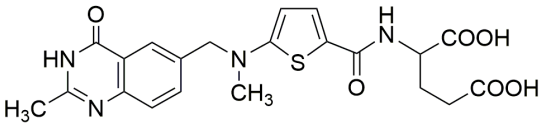

ZD1694

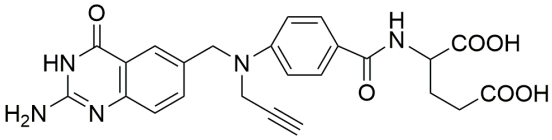

CB3717

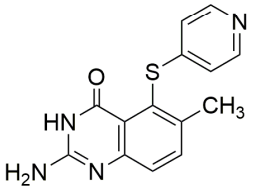

AG337

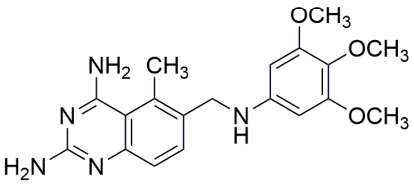

Trimetrexate

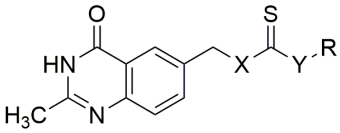

I, X = S, Y = NH
II, X = NH, Y = S

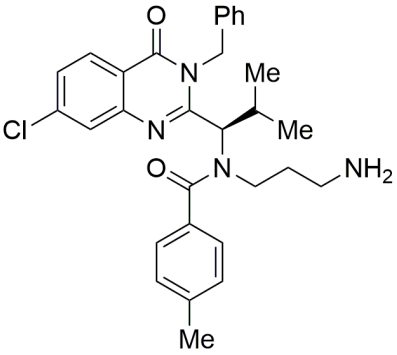

Ispinesib

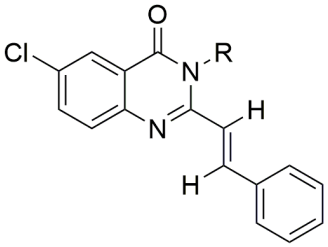

III, R = Pyrimidin-2-yl

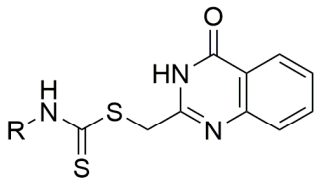

Target compounds **5a**–**t**

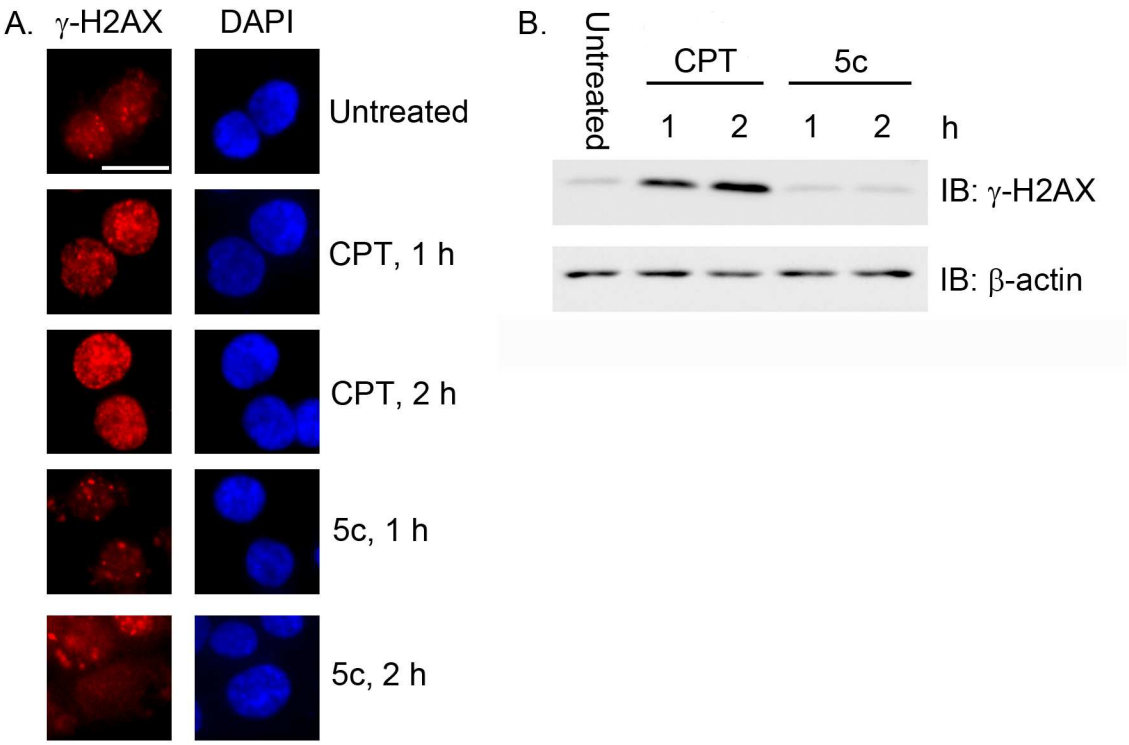

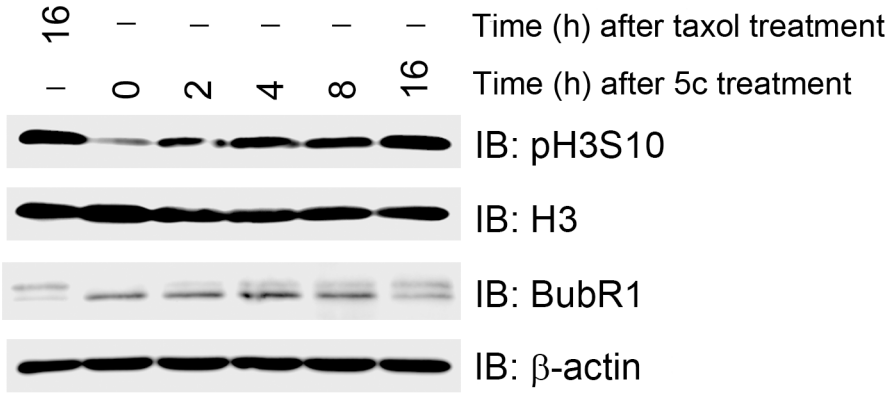

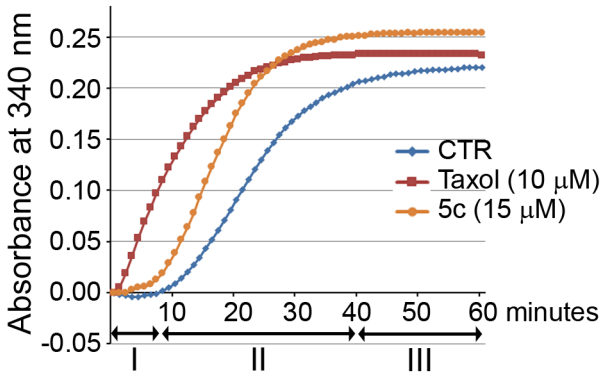

Research highlights

- Twenty dithiocarbamate derivatives of quinazolin-4(3*H*)-one were synthesized.
- Antiproliferative activities of **5a**–**t** against five cancer cell lines were evaluated.
- Compound **5c** induced a G2/M arrest in HT29 cells.
- **5c** promoted tubulin polymerization and activated the spindle assembly checkpoint.